Evidence of a natural marine source of oxalic acid and a possible link to glyoxal

Matteo Rinaldi, Stefano Decesari, Claudio Carbone, Emanuela Finessi, Sandro Fuzzi, Darius Ceburnis, Colin O'Dowd, Jean Sciare, John Burrows, Mihalis Vrekoussis, et al.

Evidence of a natural marine source of oxalic acid and a possible link to glyoxal

Matteo Rinaldi,[1] Stefano Decesari,[1] Claudio Carbone,[1] Emanuela Finessi,[1] Sandro Fuzzi,[1] Darius Ceburnis,[2] Colin D. O'Dowd,[2] Jean Sciare,[3] John P. Burrows,[4] Mihalis Vrekoussis,[4,5] Barbara Ervens,[6,7] Kostas Tsigaridis,[8,9] and Maria Cristina Facchini[1]

Received 20 January 2011; revised 26 May 2011; accepted 6 June 2011; published 26 August 2011.

[1] This paper presents results supporting the existence of a natural source of oxalic acid over the oceans. Oxalate was detected in "clean-sector" marine aerosol samples at Mace Head (Ireland) (53°20′N, 9°54′W) during 2006, and at Amsterdam Island (37°48′S, 77°34′E) from 2003 to 2007, in concentrations ranging from 2.7 to 39 ng m^{-3} and from 0.31 to 17 ng m^{-3}, respectively. The oxalate concentration showed a clear seasonal trend at both sites, with maxima in spring-summer and minima in fall-winter, being consistent with other marine biogenic aerosol components (e.g., methanesulfonic acid, non-sea-salt sulfate, and aliphatic amines). The observed oxalate was distributed along the whole aerosol size spectrum, with both a submicrometer and a supermicrometer mode, unlike the dominant submicrometer mode encountered in many polluted environments. Given its mass size distribution, the results suggest that over remote oceanic regions oxalate is produced through a combination of different formation processes. It is proposed that the cloud-mediated oxidation of gaseous glyoxal, recently detected over remote oceanic regions, may be an important source of submicrometer oxalate in the marine boundary layer. Supporting this hypothesis, satellite-retrieved glyoxal column concentrations over the two sampling sites exhibited the same seasonal concentration trend of oxalate. Furthermore, chemical box model simulations showed that the observed submicrometer oxalate concentrations were consistent with the in-cloud oxidation of typical marine air glyoxal mixing ratios, as retrieved by satellite measurements, at both sites.

Citation: Rinaldi, M., et al. (2011), Evidence of a natural marine source of oxalic acid and a possible link to glyoxal, *J. Geophys. Res.*, *116*, D16204, doi:10.1029/2011JD015659.

1. Introduction

[2] Oxalic acid is the most abundant dicarboxylic acid detected in tropospheric aerosols [*Kerminen et al.*, 1999], with concentrations ranging from a few ng m^{-3} in remote regions up to 900 ng m^{-3} in urban air [*Warneck*, 2003, and references therein].

[3] Oxalic acid has often been observed in marine aerosols, although, given the high concentrations found in polluted environments, its origin has often been attributed to transport from the continent [*Matsumoto et al.*, 1998; *Kawamura and Sakaguchi*, 1999; *Mochida et al.*, 2003a, 2003b; *Aggarwal and Kawamura*, 2008].

[4] The idea of a biogenic marine source of oxalic acid and other low-molecular-weight (LMW) dicarboxylic acids has been sporadically proposed in the literature over the years. For instance, *Kawamura et al.* [1996a, 1996b] attributed oxalic acid and other LMW dicarboxylic acids in aerosol samples over the Antarctic Ocean to the photochemical degradation of fatty acids of phytoplankton origin, transferred into the atmosphere within sea-spray particles. *Baboukas et al.* [2000] also hypothesized a marine source of oxalic acid, although much weaker than continental ones, observing some correlation between oxalic acid and methanesulfonic acid (MSA), out of main continental outflows over the Atlantic Ocean.

[1]Institute of Atmospheric Sciences and Climate, National Research Council, Bologna, Italy.
[2]School of Experimental Physics and Environmental Change Institute, National University of Ireland Galway, Galway, Ireland.
[3]Laboratoire des Sciences du Climat et de l'Environnement, CNRS-CEA-IPSL, Gif-sur-Yvette, France.
[4]Institute of Environmental Physics and Remote Sensing, University of Bremen, Bremen, Germany.
[5]Now at Research Centre for Atmospheric Physics and Climatology, Academy of Athens, Athens, Greece.
[6]Cooperative Institute for Research in Environmental Sciences, University of Colorado at Boulder, Boulder, Colorado, USA.
[7]Chemical Sciences Division, Earth System Research Laboratory, NOAA, Boulder, Colorado, USA.
[8]Center for Climate Systems Research, Columbia University, New York, New York, USA.
[9]NASA Goddard Institute for Space Studies, New York, New York, USA.

0148-0227/11/2011JD015659

[5] More recently, *Turekian et al.* [2003] presented results of compound-specific $\delta^{13}C$ analyses, evidencing a marine origin for aerosol oxalic acid in Bermuda. *Warneck* [2003] discussed a chemical mechanism indicating a natural route to the production of oxalic acid in marine clouds from biogenic gaseous precursors, namely acetylene and ethene, through the formation of glyoxal and glycolaldehyde, respectively. The importance of the atmospheric oxidation of glyoxal (and glyoxylic acid) for the formation of oxalic acid was previously discussed by *Kawamura et al.* [1996a, 1996b], although without evidencing the role of liquid-phase chemistry in the process. Measurements performed below, above, and in-cloud in the near-coast marine atmosphere [*Crahan et al.*, 2004; *Sorooshian et al.*, 2007] supported *Warneck*'s [2003] mechanism of oxalic acid production in marine clouds, even though the authors did not discuss the origin, whether natural or anthropogenic, of the gaseous precursors involved in the process. *Miyazaki et al.* [2010] suggested that substantial fractions of oxalic acid in biologically influenced marine aerosols over the western North Pacific resulted from the degradation of organic precursors emitted by sea-spray processes in oceanic regions with high biological productivity.

[6] This paper reports data supporting the existence of a natural source of aerosol oxalic acid over the oceans, also discussing the possibility that glyoxal, observed over the oceans in concentrations of the order of tens ppt, may be an important precursor of aerosol oxalic acid via in-cloud oxidation.

2. Experimental Setup

2.1. Sampling

[7] Aerosol sampling was performed at two coastal stations, one in the Northern Hemisphere, Mace Head (Ireland), facing the North Atlantic Ocean at 53°20′N, 9°54′W, and the other in the Southern Hemisphere, Amsterdam Island, located in the southern Indian Ocean sector of the Austral Ocean, at 37°48′S, 77°34′E.

[8] Sampling at Mace Head was performed throughout 2006, with an average frequency of about one sample per month (with the exception of the June-July period, when two samples per month were collected), and a sampling time of 30–100 h. Aerosol samples were collected by an eight-stage Berner low-pressure impactor, operating at 30 LPM and using tedlar foils as sampling substrates. Particle segregation was performed according to the following 50% equivalent aerodynamic cutoff diameters: 0.06, 0.125, 0.25, 0.5, 1, 2, 4, 8, 16 μm. To avoid contamination from both local sources and long-range transport of anthropogenic aerosols, a well-established clean-sector sampling strategy was adopted so that samples were collected only in unperturbed marine air masses. Details on the clean-sector aerosol sampling strategy and instrumentation can be found in previously published studies [*Facchini et al.*, 2008a; *Rinaldi et al.*, 2009]. Approximately one non-clean-sector sample (polluted samples, hereafter) per month was collected for comparison purposes.

[9] Bulk (TSP) aerosols were sampled at Amsterdam Island on a 10 day basis from May 2003 to December 2004, using an open-face filtration device (NILU, Norway) running on average at 28.4 ± 1.5 LPM with prefired 25 mm diameter quartz filters. From January 2005 to November 2007, these bulk aerosols were sampled on an 8 day basis using an open-face filtration device (NILU, Norway) running on average at 41.8 ± 0.9 LPM with prefired 47 mm diameter quartz filters. Colocated size-segregated aerosols (PM1, PM2.5, PM10, TSP) were sampled within the same sampling intervals (8 days) from January 2005 to November 2007 on preweighed Teflon filters. Aerosol size segregation was performed with a four-stage cascade impactor (Dekati Ltd) running at 30 ± 1 LPM. A detailed description of the site characteristics is provided by *Sciare et al.* [2009]. Given the remote character of the site, no clean-sector strategy was necessary to avoid local contaminations, although the site can be affected by biomass-burning aerosols transported from South Africa and Madagascar from July to September, with a maximum in August [*Sciare et al.*, 2009]. A post-sampling filtration was applied to the database, discarding all samples associated with an equivalent black carbon (EBC) value higher than 10 ngC m^{-3}, effectively excluding all anthropogenically contaminated samples. Given the strong influence of African biomass burning during the month of August, the samples collected during that month were considered "contaminated," regardless of their EBC concentration.

2.2. Analyses of Oxalate in Aerosol Samples

[10] Oxalate anion quantifications on aerosol water extracts were performed by ion chromatography at the Institute for Atmospheric Sciences and Climate, Bologna, Italy (Mace Head samples) and at the Laboratoire des Sciences du Climat et de l'Environnement, Gif-sur-Yvette, France (Amsterdam Island samples).

[11] The analytical protocol for Mace Head samples is described in detail by *Cavalli et al.* [2004] and *Facchini et al.* [2008a]. One unsampled substrate was associated with each impactor sample for blank correction. Blank oxalate levels in the tedlar substrates deployed at Mace Head were always below the detection limit (0.7 ppb).

[12] Details on the analytical protocols for Amsterdam Island samples are provided by *Sciare et al.* [2007]. Prefired quartz and Teflon filters were taken in the field on a monthly basis for blank corrections. Blank oxalate concentrations for prefired quartz filters were on average 7.9 ± 4.4 ppb while blank corrected atmospheric oxalate concentrations ranged from 13.4 to 118.5 ppb (mean, 38.4 ppb). Oxalate concentrations below the detection limit (~0.1 ppb) were observed for the blank Teflon filters.

[13] The overall error in the determination of oxalate is estimated to be of the order of 10% and takes into account the analytical accuracy and the filter blank variability (when applicable). Since ion chromatography allows the quantification of oxalate independently of its chemical form, in the following, we refer to the sum of oxalic acid and oxalate in aerosol particles as to oxalate.

2.3. Satellite Measurements of Glyoxal

[14] Six years (2003–2008) of glyoxal observations retrieved from the radiances recorded by the Scanning Imaging Absorption Spectrometer for Atmospheric Cartography (SCIAMACHY) were used in the present study. The SCIAMACHY instrument is an imaging ultraviolet-visible-near-infrared (UV-VIS-near IR) spectrometer on board the

Table 1. Average (±Standard Deviation) Oxalate Formation Rates, Calculated Between 0.5 and 3 h of Cloud Processing at Mace Head and Amsterdam Island[a]

	Glyoxal Mixing Ratio (pptv)	Oxalate Formation Rate (ng m^{-3} min^{-1})	
		pH 4	pH 6
MH_SS	187 ± 103	0.36 ± 0.11	1 ± 0.17
MH_FW	67 ± 54	0.11 ± 0.035	0.33 ± 0.057
AI_SS	101 ± 65	0.52 ± 0.13	1.2 ± 0.12
AI_FW	34 ± 47	0.16 ± 0.043	0.38 ± 0.038

[a]Input glyoxal mixing ratios are also reported. MH, Mace Head; AI, Amsterdam Island; FW, fall-winter; SS, spring-summer.

ESA Envisat satellite [*Burrows et al.*, 1995; *Gottwald et al.*, 2006]. Envisat flies in a sun-synchronous near-polar orbit. It has a nominal ground pixel size of 30 km along track and 60 km across track (60 × 30 km) and the total across-track footprint provides global coverage every 6 days. The local equator overpass time is around 10:00 A.M. local time.

[15] The analysis of the vertical columns of glyoxal (VC_{GLY}) involved the following steps: (1) Differential optical absorption spectroscopy (DOAS) [*Platt*, 1994] was used to retrieve the glyoxal slant column densities (SC_{GLY}). Details on the retrieval method are provided by *Vrekoussis et al.* [2009]; (2) the SC_{GLY} were converted to VC_{GLY} using the air mass factor (AMF) calculations based on the radiative transfer model SCIATRAN [*Rozanov et al.*, 2005], accounting for the average light path length in the atmosphere.

[16] It should be noted that assumptions were made for the a priori realistic conditions of the atmosphere. However, the AMF based on the real conditions of the atmosphere may differ from the a priori AMF, with a potential impact on the reported VC_{GLY}. The largest error is introduced by potential differences between the real aerosol profile and the existence of residual clouds, which are considered to be less than 20% [*Vrekoussis et al.*, 2009]. Both the aerosol vertical distribution and aerosol type (e.g., urban versus maritime) will affect visibility and, hence, the photon light path. However, given the lack of information on the vertical distribution of aerosols, any attempt at a correction for aerosol effects would be speculative at this point. For the residual clouds, two extreme scenarios can be considered: (1) All glyoxal is found under the clouds, and, as a result, cloud shielding in the lower troposphere will lead to glyoxal underestimation; and (2) all glyoxal is found above a cloud's top height, so that the high surface reflectance will lead to glyoxal overestimation. The latter case is expected to be a rare possibility.

[17] Future improvement on the retrieval algorithms will take into account the synergistic measurements of aerosol and clouds performed by the other instruments aboard Envisat. A detailed discussion regarding the impact of clouds and aerosol distribution on the glyoxal AMF computation is given by *Vrekoussis et al.* [2009, 2010].

[18] For the present study the monthly mean values of VC_{GLY} were retrieved over Mace Head and Amsterdam Island and the extended area of 500 km around their central longitudes and latitudes.

2.4. Chemical Box Model

[19] A box model has been developed that includes a reaction scheme based on laboratory and model studies [*Ervens et al.*, 2003a, 2004] and represents glyoxal oxidation by the OH radical in the aqueous phase of cloud droplets. The uptake of glyoxal and OH is described by a kinetic approach; no OH liquid-phase formation pathways are considered. Glyoxal is oxidized to oxalic acid in a two-step reaction pathway with glyoxylic acid as an intermediate compound. The oxidation of both glyoxylic acid and oxalic acid is pH dependent, with higher rate constants for the dissociated forms [*Ervens et al.*, 2003b].

[20] The aqueous phase reactions considered in the model are summarized as follows:

$$\mathrm{OH} + \mathrm{glyoxal} \rightarrow \mathrm{glyoxylic\ acid/glyoxylate}, \quad (1)$$

$$\mathrm{glyoxylic\ acid/glyoxylate} + \mathrm{OH} \rightarrow \mathrm{oxalic\ acid}, \quad (2)$$

$$\mathrm{oxalic\ acid/oxalate} + \mathrm{OH} \rightarrow \mathrm{CO_2}. \quad (3)$$

[21] The box model does not include any microphysical processes (cloud formation or evaporation). Clouds are presented by a constant liquid water content (LWC) of 0.1 g m^{-3}, this being of a typical order of magnitude for marine stratocumulus clouds. Since no measurements of cloud fractions were available from the experiments, cloud-processing times between 0.5 and 3 h were considered, as they are representative for cloud processing in multiple cloud cycles.

[22] The chemical concentrations of the gas-phase species glyoxal and the OH radical were maintained constant throughout the simulation period, implying a continuous source. OH concentrations of 10^6 and 3×10^6 cm^{-3} were assumed at both locations to simulate oxalate production in fall-winter and spring-summer, respectively. These OH concentrations and seasonal trends are in agreement with previous OH measurements at similar locations (e.g., *Monks et al.*, [2000]). The glyoxal concentration is constrained by satellite measurements (see previous section). To convert the column density satellite retrievals into actual concentrations, use was made of the AR5 version of the GISS model E general circulation model. The model ran with the year 2000 anthropogenic emissions and allowed the calculation of climate variability. Five years of simulations (after a year of spin-up) were sampled daily at 10:00 A.M. local time and averaged per month in order to obtain the average climatology of the boundary-layer height at Mace Head and Amsterdam Island, along with as the standard deviation of its variability during the 5 year simulation. These boundary-layer heights were used in the conversion of glyoxal columnar densities to number densities (molecules cm^{-3}), assuming that all glyoxal is well mixed within the boundary-layer height and that 1 pptv of glyoxal is equal to 2.45×10^7 molecules cm^{-3} for pressure $P = 1$ atm and temperature $T = 25°C$. Average fall-winter and spring-summer mixing ratios were computed at both sites based on the above mentioned calculations (Table 1).

3. Results

3.1. Oxalate in Marine Aerosols

[23] Oxalate was detected in marine air masses at Mace Head and Amsterdam Island in concentrations from 2.7 to 39 ng m^{-3} and from 0.31 to 17 ng m^{-3}, respectively. As shown in Figure 1, oxalate concentrations followed a clear

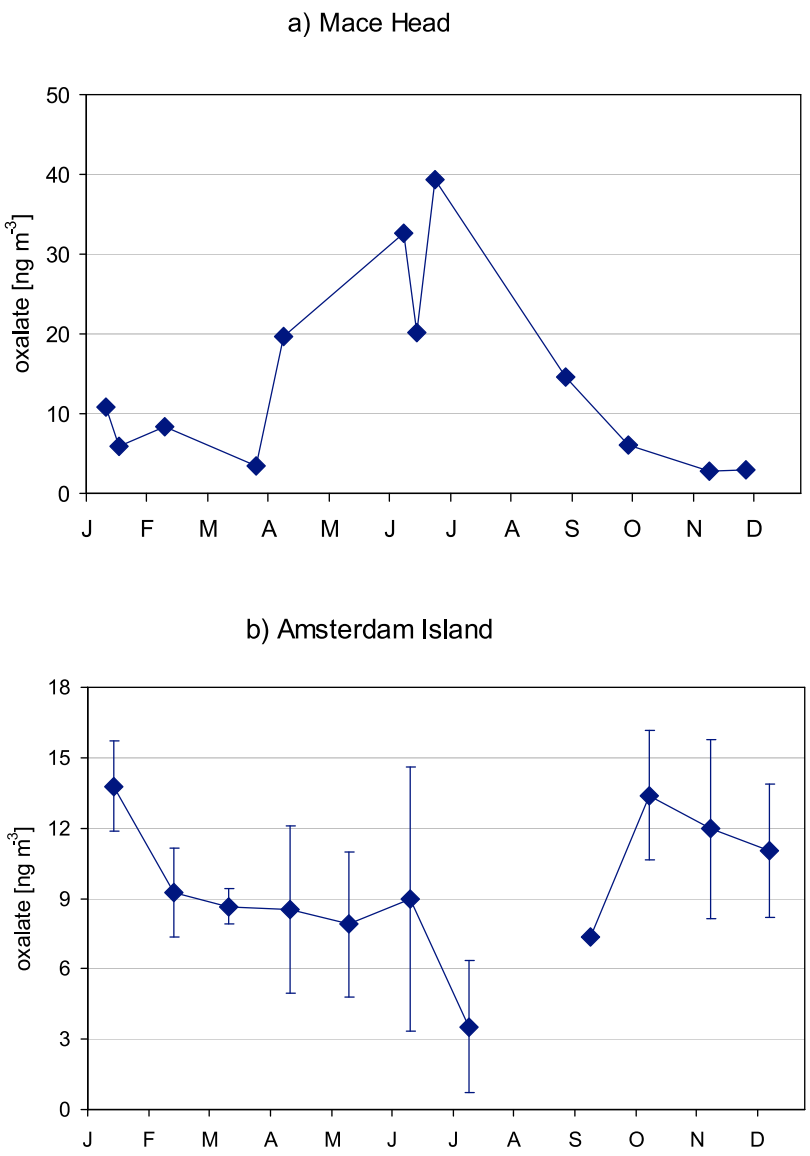

Figure 1. Observed oxalate concentrations as a function of time at (a) Mace Head (PM_8) and (b) Amsterdam Island (TSP). Data points represent single samples collected in 2006 for Mace Head and monthly averages from 2003 to 2007 for Amsterdam Island (the bars represent ±1 standard deviation), after the postsampling filtration.

seasonal trend at both sites, with maxima in the spring-summer period and minima in the fall-winter period. The spring-summer oxalate concentration was significantly higher ($p < 0.01$) than the fall-winter one, with 25 ± 10 versus 5.7 ± 3.0 ng m^{-3} and 11 ± 3.0 versus 7.2 ± 4.0 ng m^{-3} at Mace Head and Amsterdam Island, respectively. The trend closely follows the yearly cycle of oceanic biological activity, which is characterized by the highest productivity during the period from spring through fall and by a quiescent period during the cold season [*Cavalli et al.*, 2004; *O'Dowd et al.*, 2004; *Sciare et al.*, 2009]. The seasonal trend is typical of biogenic components of marine aerosols, such as MSA, non-sea-salt (nss) sulfate [*Cavalli et al.*, 2004], and ammonium and alkylammonium salts [*Facchini et al.*, 2008a], suggesting, also for oxalate, the presence of a natural source in the MBL.

[24] A similar contribution of oxalate carbon (C_{oxa}) to total organic carbon (OC) was observed at the two sites, with average values of 1.6% ± 0.8% at Mace Head and and 2.2% ± 1.0% at Amsterdam Island. Assuming that all observed aerosol oxalates are of marine origin, the similarity of the C_{oxa}/OC ratio at the two sites suggests that the oxalate source has the same relative strength with respect to the other marine organic aerosol sources. Amsterdam Island is generally characterized by lower aerosol mass concentrations than Mace Head, as already documented by *Sciare et al.* [2009]. The present C_{oxa}/OC ratios are fairly consistent with those reported by *Kawamura et al.* [2010] (0.5%–3.5%) and *Miyazaki et al.* [2010] (0.6%–1.0%) for Arctic Ocean and North Pacific Ocean aerosols, respectively. Moreover, *Kawamura and Sakaguchi* [1999] reported C_{oxa}/OC ratios from less than 1% to 10% over the Pacific Ocean, with the greater contributions at tropical latitudes.

[25] In clean marine samples, oxalate was distributed along the whole size spectrum (Figure 2), with the submicrometer

fraction contributing 46% ± 15% and 33% ± 18% of the oxalate mass at Mace Head and Amsterdam Island, respectively. The largest contribution in the submicrometer fraction was observed at Mace Head in the 0.25–0.5 μm size range (22% ± 9%), while this information was not available for Amsterdam Island because of the lower resolution of the sampling device. As for the supermicrometer fraction, the largest contribution was observed in the 1.0–2.0 μm size range at Mace Head and in the 1.0–2.5 μm size range at Amsterdam Island.

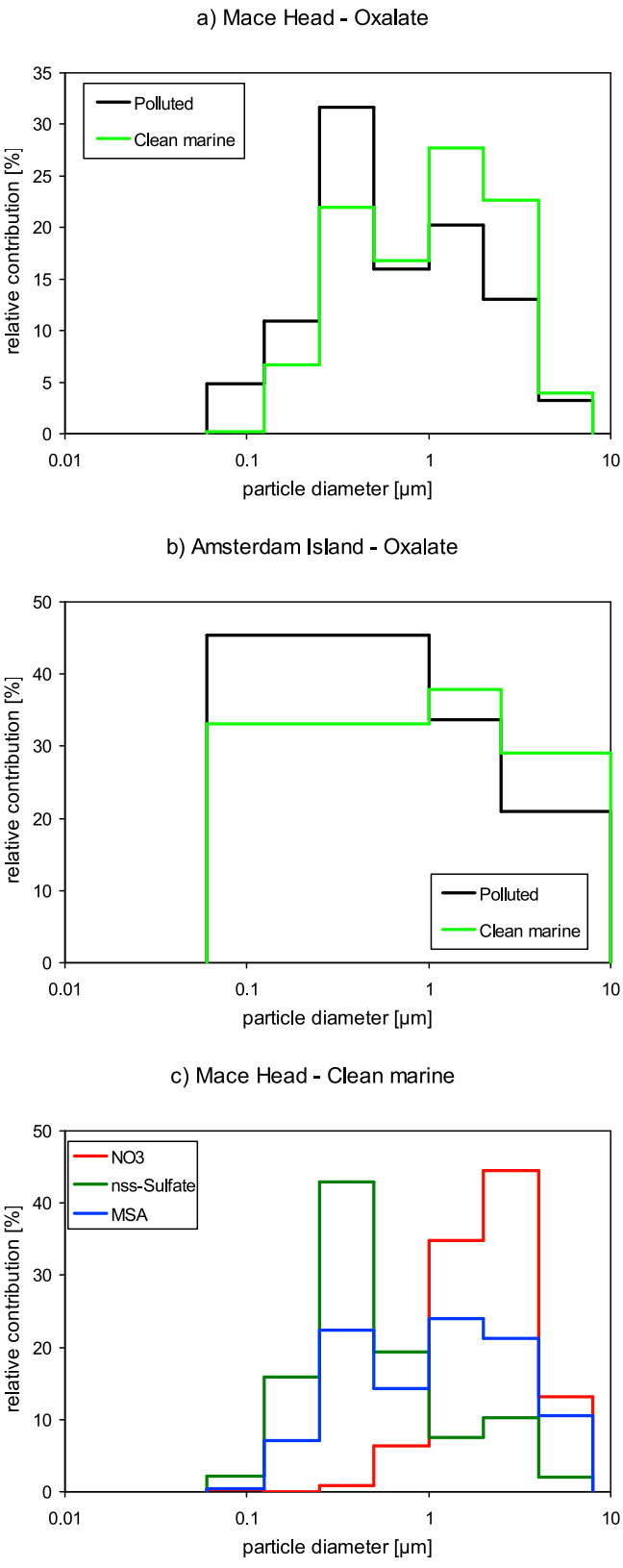

[26] It is also worth noting that the oxalate size distribution in clean marine samples observed at Mace Head differs from that of nitrate (Figure 2c), with 79% of its mass in the 1.0–4.0 μm size range, and from that of nss sulfate, which is mainly present in the submicrometer fraction (80% of the mass). By contrast, it closely resembles the MSA size distribution, which is characterized by almost equivalent submicrometer and supermicrometer modes.

[27] The samples collected at Mace Head under continental influence conditions (polluted samples) showed a different oxalate mass size distribution, peaking in the accumulation mode, with 63% of the oxalate mass accounted for by the submicrometer fraction. Samples collected at Amsterdam Island during August and September under the influence of South African biomass-burning events [*Sciare et al.*, 2009], exhibited a mass peak in the submicrometer range. This observation is coherent with previous studies, where oxalate is observed to undergo a shift toward larger diameters in clean marine samples as compared with polluted ones [*Matsumoto et al.*, 1998; *Kerminen et al.*, 1999]. The latter present an oxalate distribution consistent with those observed in continental polluted areas [*Kerminen et al.*, 2000; *Yao et al.*, 2002; *Hsieh et al.*, 2007], suggesting that the difference cannot be attributed to the preferential removal of coarse particles during the advection of continental air masses over the open ocean. The size distribution difference between clean marine and polluted samples strongly suggests a different formation pathway, or a combination of different formation routes, over remote oceanic regions.

[28] *Mochida et al.* [2003b] proposed the preferential partitioning of oxalate into coarse particles, because of the mildly alkaline properties of supermicrometer marine aerosols, as for nitrate, to explain the distribution of oxalate in marine aerosols. However, the different size distributions observed for nitrates at Mace Head during 2006 suggest that this hypothesis alone cannot explain the complexity of oxalate mass size distribution. According to *Kerminen et al.* [1999], the lower supermicrometer oxalate mode (geometric mean diameter at 2 μm) could be formed by condensation from the gas phase (hypothesis also considered by *Turekian et al.* [2003]), by heterogeneous reactions between a precursor compound and sea-salt particles, or in cloud droplets. Indeed, there is growing evidence from atmospheric observations that oxalate is a product of cloud processing [*Chebbi and Carlier*, 1996; *Ervens et al.*, 2003a, 2004; *Crahan et al.*, 2004; *Yu et al.*, 2005; *Carlton et al.*, 2007]. In particular, the studies of *Warneck* [2003], *Crahan et al.* [2004], *Sorooshian et al.* [2006], and, more recently, *Miyazaki et al.* [2010] demon-

Figure 2. Observed average normalized size distribution of (a) oxalate at Mace Head in clean marine and polluted samples, (b) oxalate at Amsterdam Island in clean marine and polluted samples, and (c) nitrate, nss sulphate, and MSA at Mace Head in clean marine samples for comparison purposes. The average concentration of the aerosol component in each stage is normalized to the total concentration of the component.

strate the potential importance of this formation pathway in the MBL. In addition, observations on aged dust particles suggest that oxalate and other highly oxidized compounds can be formed in the aqueous phase of deliquesced particles [*Yao et al.*, 2002], although, in such highly concentrated solutions, highly oxidized polymeric compounds are expected to be favored, with oxalate remaining a minor product [*Tan et al.*, 2009; *Ervens and Volkamer*, 2010]. As for the gas-phase production of oxalate, no reaction is currently known [*Warneck*, 2003], and the process is considered unlikely. Finally, the photochemical oxidation of biogenic unsaturated fatty acids, enriched in sea-spray particles produced from biologically active waters [*Keene et al.*, 2007; *Facchini et al.*, 2008b], could be a potential source of oxalate in clean marine aerosol [*Matsumoto et al.*, 1998; *Kawamura and Sakaguchi*, 1999; *Turekian et al.*, 2003; *Miyazaki et al.*, 2010].

[29] A direct emission of oxalate from oceanic water by sea-spray processes can be also hypothesized, although recent studies have shown that water-insoluble, low-oxidized biomolecules rather than water-soluble species (such as oxalate) are preferentially transferred from the sea surface by sea spray [*Facchini et al.*, 2008b; *Miyazaki et al.*, 2010]. Moreover, *Miyazaki et al.* [2010] recently concluded that oxalate is mainly secondary over the Pacific Ocean, far from continental outflows, given the systematic lack of correlation between this aerosol component and Na^+.

[30] The oxalate mass size distribution observed in clean marine air masses probably results from a combination of the above secondary processes, with in-cloud processes mainly contributing to the submicrometer fraction. It has been shown that cloud processing leads to a relatively larger mass production of submicrometer particles that is due to their relatively high contribution to the total mass and hence to liquid water in clouds [*Feingold and Kreidenweis*, 2000; *Ervens et al.*, 2004]. The condensation of gaseous oxalic acid mainly contributes to the coarse-mode oxalate, as a result of the higher pH of coarse particles in marine aerosol [*Keene et al.*, 1998, 2002, 2004] favoring the formation of stable salts. The volatilization from fine particles, in which oxalic acid formed in clouds may be only partially stabilized as oxalate salts, because of the lower pH, can be an important source of gas-phase oxalic acid, able to subsequently condense on coarse particles. As a consequence, in-cloud processes may also be indirectly responsible for supermicrometer oxalate. The photochemical oxidation of a biogenic primary organic aerosol may potentially contribute to both the submicrometer and supermicrometer aerosol fractions, as primary organics have been observed in comparable concentrations throughout the whole size spectrum [*Facchini et al.*, 2008b].

[31] The hypothesis of a multiprocess origin for oxalate is also supported by the similarity observed between its mass size distribution and that of MSA. In fact, MSA and nss sulfate are both oxidation products of biogenic dimethyl sulfide (DMS) in the MBL, although they present different size distributions as a function of the different formation routes. Nss sulfate derives mainly from in-cloud oxidation of DMS-derived SO_2 and from new particle-formation events involving gas-phase H_2SO_4 [*Von Glasow and Crutzen*, 2004; *Barnes et al.*, 2006; *Hopkins et al.*, 2008], resulting in a narrow accumulation mode peaked size distribution. The formation of MSA in a marine aerosol follows a number of parallel routes, involving the adsorption of gas-phase-produced MSA onto sea-salt particles, but also the multistep oxidation in clouds or particles of organosulfur DMS oxidation intermediates, like dimethyl sulfoxide and methanesulfinic acid [*Bardouki et al.*, 2002; *Von Glasow and Crutzen*, 2004; *Barnes et al.*, 2006]. As a result, MSA typically presents a broad size distribution, with a significant supermicrometer fraction [*Hopkins et al.*, 2008].

3.2. A Hypothesis for the Origin of Submicrometer Oxalate Related to Glyoxal

[32] With regard to in-cloud-mediated production, this paper suggests that glyoxal may be an important oxalate precursor in the MBL. In fact, a natural source of gaseous glyoxal, one of the main known oxalate precursors via in-cloud oxidation [*Ervens et al.*, 2004; *Lim et al.*, 2005; *Carlton et al.*, 2007], has recently been discovered over remote oceanic regions from modeling studies [*Fu et al.*, 2008; *Myriokefalitakis et al.*, 2008], ground-based observations [*Sinreich et al.*, 2010], and satellite measurements [*Wittrock et al.*, 2006; *Vrekoussis et al.*, 2009, 2010].

[33] The origin of glyoxal in the MBL is still matter of debate, and it is beyond the scope of this paper to fill the present knowledge gap. Nevertheless, given its short atmospheric lifetime (2–3 h) [*Myriokefalitakis et al.*, 2008], it is clear that the concentrations observed over remote oceanic regions cannot be attributed merely to transport from land. As for MBL sources, an interesting mechanism has recently been proposed for the photodegradation of chlorophyll (as a proxy for marine organic matter) in the presence of ozone at the air-sea interface [*Reeser et al.*, 2009a, 2009b], one that could explain the formation of volatile organic products like glyoxal. However, the high solubility of glyoxal is expected to determine a preferential diffusion from the sea surface microlayer into the bulk seawater rather than its volatilization into the atmosphere [*Zhou and Mopper*, 1990, 1997], unless unrealistically high concentrations of glyoxal are assumed in surface seawaters. This leads to the conclusion that the most likely source of glyoxal is the MBL, even though it remains unclear whether it is due to gas-phase reactions [e.g., *Warneck*, 2003] or to heterogeneous chemistry in aerosols or clouds.

3.2.1. Satellite Measurements of Glyoxal

[34] Supporting the hypothesis that glyoxal is an important oxalate precursor in the MBL, Figure 3 shows SCIAMACHY satellite-retrieved glyoxal column concentrations over the two sampling sites, demonstrating a clear seasonal trend for the concentration of gas-phase glyoxal, similar to that of aerosol oxalate (Figure 1). Maximum column concentrations were observed over Mace Head between June and August, with an average spring-summer period concentration of 3.2×10^{14} molecules cm^{-2}, while the minimum was observed in January, with an average concentration for the fall-winter period of 1.6×10^{14} molecules cm^{-2}. At Amsterdam Island the maximum concentration was observed in December, with an average spring-summer period concentration of 2.2×10^{14} molecules cm^{-2} and an average concentration for the fall-winter period of 0.78×10^{14} molecules cm^{-2}. According to the calculations presented in section 2.4, average concentrations of 67 ± 54 and 187 ± 103 pptv were found for Mace Head in fall-winter and spring-summer conditions, respectively, while mixing ratios of 34 ± 47 and 101 ± 65 pptv were calculated for Amsterdam Island in fall-winter and spring-summer conditions, respectively. The uncertainty ranges associated with the above glyoxal mixing ratios derive

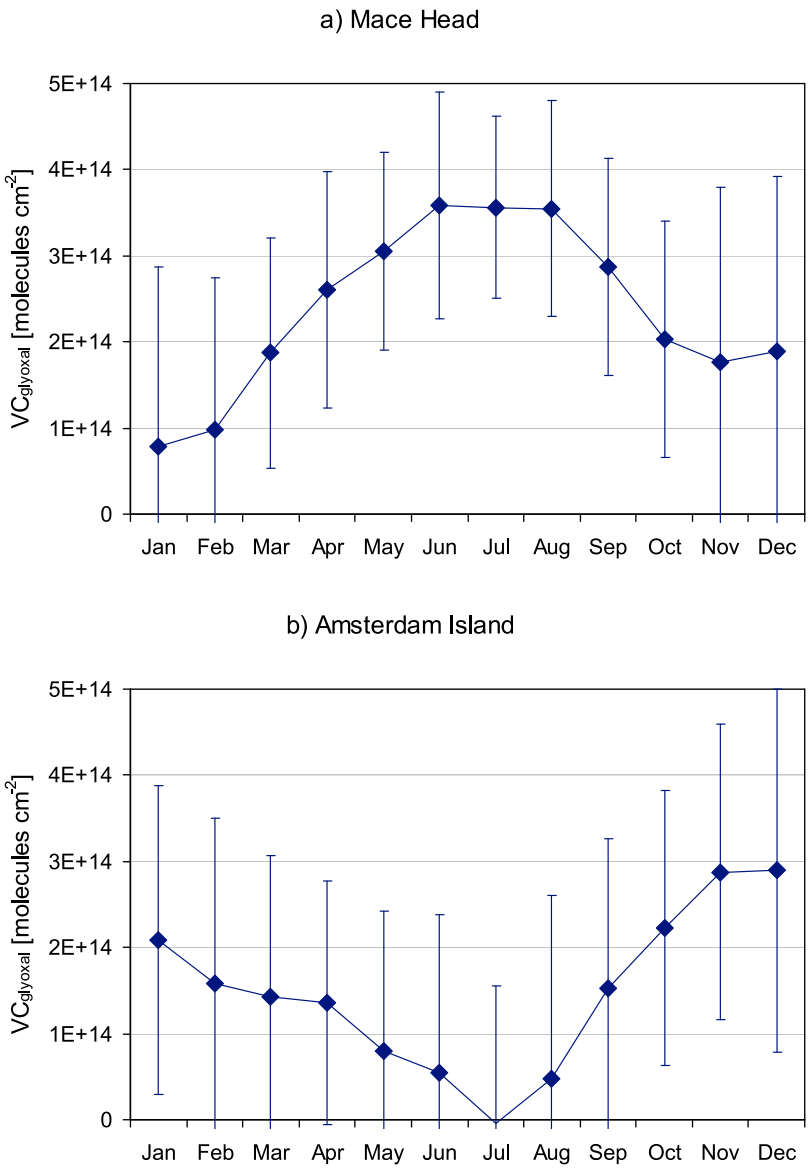

Figure 3. Monthly average SCIAMACHY satellite retrieved glyoxal column concentration around (a) Mace Head and (b) Amsterdam Island. Error bars represent the standard deviation associated with the monthly averages.

from the error affecting the satellite measurements [*Vrekoussis et al.*, 2010] combined with the variability of the MBL height computation results.

[35] Glyoxal mixing ratios measured at Mace Head and Amsterdam Island are fairly consistent with previous measurements performed in the MBL: *Zhou and Mopper* [1990] reported 80 pptv as the typical glyoxal concentration over the open Caribbean Sea and Sargasso Sea, while *Sinreich et al.* [2007, 2010] presented concentrations ranging between 75 and 350 pptv for the gulf of Maine and between 25 and 140 pptv over the remote tropical Pacific Ocean. For comparison, glyoxal mixing ratios measured in Tokyo urban air range between 30 and 700 pptv (average 170) [*Okuzawa et al.*, 2007].

3.2.2. Modeling of Oxalate Formation

[36] To test the hypothesis of the role of gas-phase glyoxal as a precursor of particulate oxalate, a chemical box model was deployed (section 2.4), using the above glyoxal mixing ratios as input data. Aerosol oxalate concentrations resulting from model simulations are reported in Figure 4 and Table 1. The nominal size cut of the predicted oxalate concentrations is 2 μm, even if most of the modeled oxalate is submicrometer. Generally, higher oxalate concentrations are predicted in spring-summer conditions than in the fall-winter period, since the oxalate formation rates are higher because of higher OH concentrations. Results are shown for pH 4 and pH 6, this being a typical range for cloud droplets in clean (marine) scenarios [*Graedel and Weschler*, 1981; *Collett et al.*, 1994]. Higher oxalate concentrations are predicted at higher pH, since the rate constant of the oxalate loss is significantly lower at higher pH, when oxalate is present in its monoanion or completely dissociated form.

[37] Based on the model results, average oxalate formation rates between 0.5 and 3 h of cloud-processing time (the sum

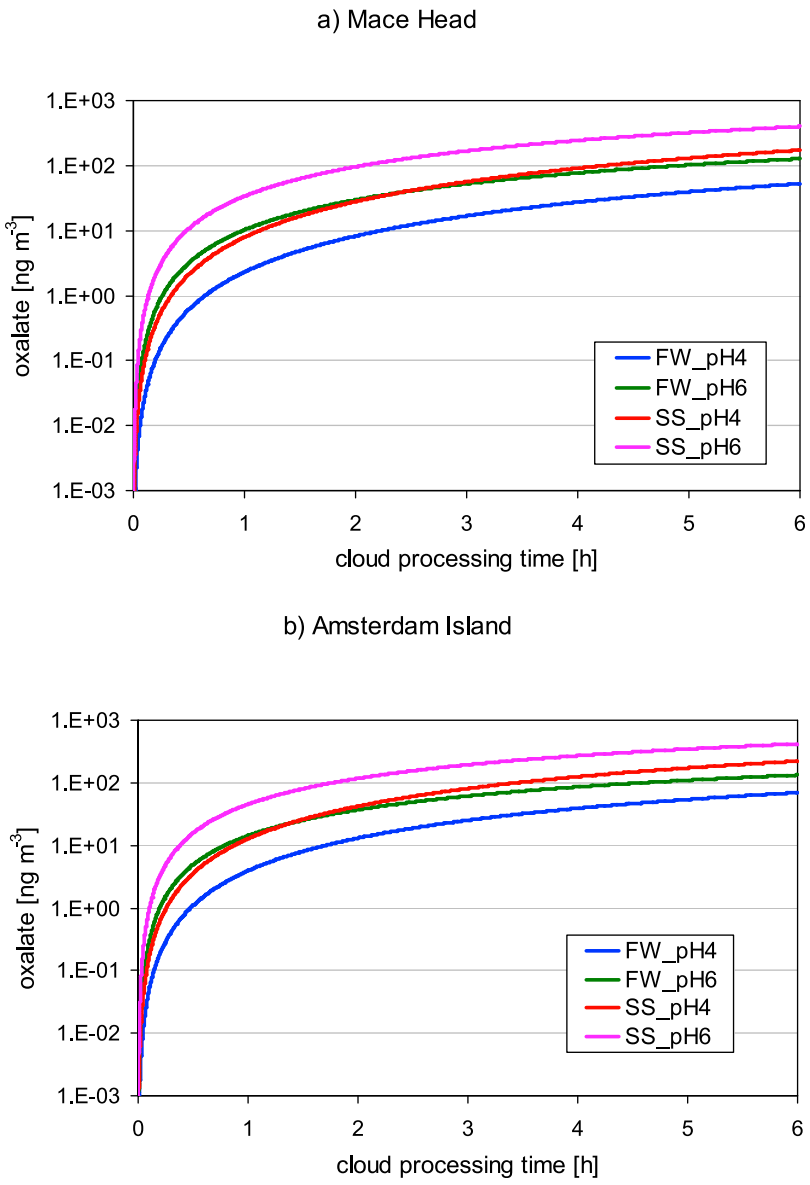

Figure 4. Modeled oxalate concentration as a function of cloud-processing time at (a) Mace Head and (b) Amsterdam Island. FW, fall-winter; SS, spring-summer.

of the time an air parcel spends in a cloud over several days) have been calculated (Table 1). Previous model studies showed that the net oxalate production slows down after several cloud cycles, since oxalate can be efficiently oxidized to CO_2. In the present case, the highest oxalate production rate is observed for Amsterdam Island in spring-summer conditions (pH 6). In these conditions, the maximum net production rate is reached after ~3 h of cloud-processing time.

[38] The results in Figure 4 reveal that the predicted oxalate concentrations are not directly proportional to the initial gas-phase glyoxal concentrations. Such effects can be explained by the more efficient OH removal by glyoxal in the aqueous phase as compared with the oxidation of glyoxylic acid or oxalate. The transport of OH into the aqueous phase is not fast enough to replenish its concentration there, and a high glyoxal concentration leads to a relatively low oxalate formation rate. According to the model results, in-cloud oxalate formation from glyoxal is therefore an oxidant-limited process. Actually, this conclusion might be due to the limited number of chemical processes in the box model employed, which does not take into account any additional (aqueous phase) OH sources (e.g., H_2O_2, Fe). However, it has been shown that OH in the aqueous phase is mostly consumed by other organic compounds [*Ervens et al.*, 2003a]. Since their concentrations cannot be constrained in the present model study, both OH(aq) source and sink terms are associated with great uncertainty. Because no observational data are available to constrain such processes, both oxalate production and loss rates might be biased, and a comparison with observations should be made on the basis of common trends and orders of magnitude, rather than an accurate reproduction of measured oxalate concentrations.

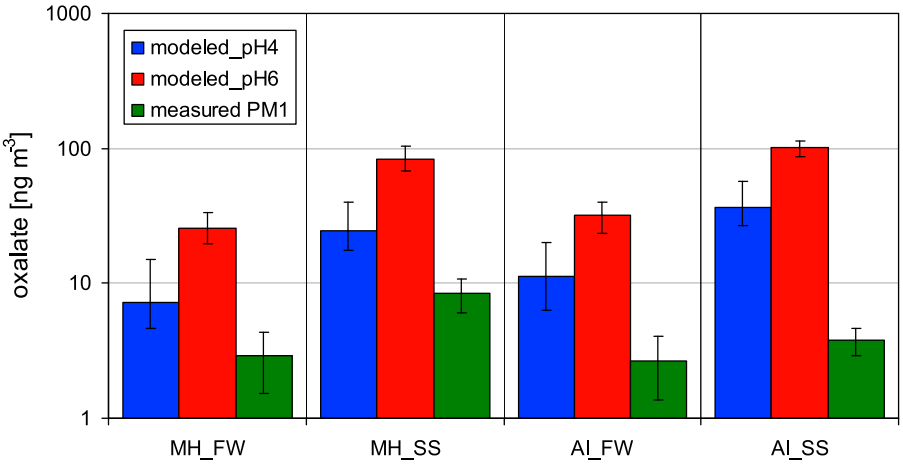

Figure 5. Predicted and observed submicrometer aerosol oxalate concentrations at Mace Head (MH) and Amsterdam Island (AI). FW, fall-winter; SS, spring-summer. The error bars associated with the model predictions represent the model output variability as a consequence of the uncertainty in glyoxal input data; the error bars associated with the measurements represent ±1 standard deviation. For Amsterdam Island, oxalate submicrometer concentration is an estimation, based on the submicrometer oxalate contribution in a subset of size-segregated samples.

[39] No information is available on cloud LWC and cloud fractions close to the sampling locations. Absolute oxalate production rates will be enhanced in a greater reaction volume (LWC) and with an extended in-cloud processing time. While a cloud over several hours (as assumed in the highly simplified model approach applied here) is not realistic, a prolonged processing time reflects several subsequent cloud cycles (several minutes each), with the assumption that oxalate mostly remains in the particle phase upon drop evaporation, forming stable salts, as suggested by *Baboukas et al.* [2000]. This assumption cannot be verified, and the evaporation between subsequent cloud cycles cannot be quantified. It is therefore likely that the model predictions overestimate in-cloud oxalate production.

[40] Measured submicrometer oxalate concentrations and the model predictions are compared in Figure 5, where the model results are averaged between 0.5 and 3 h of total cloud-processing time to give a reasonable atmospheric concentration value. The comparison can be made only roughly and only in terms of order of magnitude, as the chemical box model does not include the dynamic atmospheric processes affecting oxalate concentrations measured at the sampling point. Real concentrations are expected to be lower than those predicted by chemical modeling alone, as a result of aerosol dilution within the MBL after formation in cloud layers and of removal processes.

[41] The model output is generally consistent with the above considerations, with modeled oxalate concentrations being from 2.5 to 25 times higher than measured submicrometer oxalate concentrations in the atmosphere. Such differences can be reasonably attributed to aerosol dilution within the MBL after formation in cloud layers and to removal processes; oxalic acid overprediction that is due to the above discussed model assumptions may also contribute.

[42] This result supports the hypothesis that a significant fraction of the submicrometer oxalate observed over remote oceanic regions derives from the in-cloud oxidation of glyoxal. Unfortunately, given the uncertainties involved in the determination of the precursor concentrations and the limits of the modeling approach itself, the results do not allow a more quantitative determination of the contribution of in-cloud glyoxal oxidation with respect to other parallel submicrometer oxalate production routes.

[43] The fact that the formation of oxalate from in-cloud glyoxal oxidation appears to be an oxidant-limited process has important implications for SOA formation in the MBL. Indeed, only a small portion (~5%) of the glyoxal available in marine clouds is oxidized to produce oxalate, as shown by the model results. In fact, recent laboratory studies [*Liggio et al.*, 2005; *Carlton et al.*, 2007; *Galloway et al.*, 2009; *Shapiro et al.*, 2009; *Ervens and Volkamer*, 2010] have shown that glyoxal uptake into aqueous particles leads to the efficient formation of high-molecular-weight, multifunctional organic compounds, contributing to SOA mass by additional aqueous-phase oxidation pathways. Even though the aqueous volume of particles is much smaller than the LWC of clouds, it has been suggested that, compared with cloud droplets, more efficient processes occur in the aqueous phase of wet particles, which might determine similarly high SOA yields from glyoxal [*Ervens and Volkamer*, 2010]. This implies that glyoxal, in the MBL, can act as a source of both submicrometer oxalate and other SOAs.

4. Conclusions

[44] Aerosol measurements performed at Mace Head (Northern Hemisphere) and Amsterdam Island (Southern Hemisphere) support the existence of a natural source of oxalate over the oceans. Oxalate represents an omnipresent aerosol component in unperturbed marine air masses, and it is characterized by the typical seasonal trend in the concentration of marine aerosol biogenic components (maxima in spring-summer and minima in winter).

[45] Several formation processes can explain the presence of oxalate in marine aerosol. In-cloud oxidation of gaseous precursors and the degradation of primary biogenic organic

matter, emitted within sea spray, have been indicated in the literature as potentially important sources of oxalate in the marine boundary layer. Additionally, the neutralization of gaseous oxalic acid onto sea-salt particles may play a role.

[46] As for in-cloud sources, several precursors have been suggested based on laboratory studies (e.g., glyoxal, methylglyoxal, glycolaldehyde, and ethene, through glycolic acid [*Warneck*, 2003, *Tan et al.*, 2009; *Perri et al.*, 2009]). This paper investigated the role of glyoxal as a precursor for the in-cloud production of oxalate mainly because of the important natural source of glyoxal recently discovered in the marine boundary layer. Furthermore, the lack of gas-phase precursor measurements at the described locations limited the possibility of investigating the contribution of other precursors.

[47] This paper suggests that the in-cloud oxidation of gaseous glyoxal may be an important source of submicrometer oxalate in the marine boundary layer. Satellite measurements and chemical cloud box model predictions support this hypothesis, showing that, over the oceans, glyoxal shares the same seasonal concentration trend as aerosol oxalate and that the observed submicrometer oxalate concentrations are consistent with the in-cloud oxidation of typical marine boundary layer glyoxal mixing ratios.

[48] The model also suggests that only a small amount of the glyoxal available in cloud droplets is oxidized to oxalate, due to the kinetic limitation of oxidant (OH) uptake into cloud droplets. This implies that glyoxal in the marine boundary layer is also available for other reactions or processes. For instance, it can be oxidized in the aqueous phase of wet aerosol particles, producing high-molecular-weight SOAs by virtue of the different aqueous-phase concentration regimes with respect to cloud droplets. Thus further investigation of the different glyoxal aqueous-mediated oxidation routes in the MBL is desirable in the future to better characterize the still poorly understood marine SOA sources.

[49] Other observations are also necessary for an improved characterization of the marine oxalate source on a regional scale, as marine biogenic productivity undergoes high interannual variability [*Sciare et al.*, 2000; *Rinaldi et al.*, 2010], potentially determining considerable changes in the contribution of the marine oxalate source from one year to the next.

[50] **Acknowledgments.** The experimental work performed at Mace Head was supported by the EU Project MAP (Marine Aerosol Production) and the Irish EPA project EASI-AQCIS (Exchange at the Air-Sea Interface: Air Quality and Climate Impacts). ACCENT (Atmospheric Composition Change the European Network of Excellence) is also gratefully acknowledged. Results obtained at Amsterdam Island were supported by the French Polar Institute (IPEV) within the AEROTRACE project. Barbara Ervens acknowledges funding from the U.S. Department of Energy (BER), ASP program, grant DE-FG02-08ER64539. Mihalis Vrekoussis acknowledges the A. von Humboldt Foundation and the European Union (Marie Curie, EIF and RG) for the consecutive research fellowships.

References

Aggarwal, S. G., and K. Kawamura (2008), Molecular distributions and stable carbon isotopic compositions of dicarboxylic acids and related compounds in aerosols from Sapporo, Japan: Implications for photochemical aging during long-range atmospheric transport, *J. Geophys. Res.*, *113*, D14301, doi:10.1029/2007JD009365.

Baboukas, E. D., M. Kanakidou, and N. Mihalopoulos (2000), Carboxylic acids in gas and particulate phase above the Atlantic Ocean, *J. Geophys. Res.*, *105*(D11), 14,459–14,471, doi:10.1029/1999JD900977.

Bardouki, H., M. Barcellos Da Rosa, N. Mihalopoulos, W. U. Palm, and C. Zetzsch (2002), Kinetics and mechanism of the oxidation of dimethylsulfoxide (DMSO) and methanesulfinate (MSIA) by OH radicals in aqueous medium, *Atmos. Environ.*, *36*, 4627–4634, doi:10.1016/S1352-2310(02)00460-0.

Barnes, I., J. Hjorth, and N. Mihalopoulos (2006), Dimethyl sulfide and dimethyl sulfoxide and their oxidation in the atmosphere, *Chem. Rev.*, *106*(3), 940–975, doi:10.1021/cr020529+.

Burrows, J., E. Holzle, A. P. H. Goede, H. Visser, and W. Fricke (1995), SCIAMACHY - Scanning imaging absorption spectrometer for atmospheric chartography, *Acta Astronaut.*, *35*(7), 445–451, doi:10.1016/0094-5765(94)00278-T.

Carlton, A. G., B. J. Turpin, K. E. Altieri, S. Seitzinger, A. Reff, H.-J. Lim, and B. Ervens (2007), Atmospheric oxalic acid and SOA production from glyoxal: Results of aqueous photooxidation experiments, *Atmos. Environ.*, *41*(35), 7588–7602, doi:10.1016/j.atmosenv.2007.05.035.

Cavalli, F., et al. (2004), Advances in characterization of size-resolved organic matter in marine aerosol over the North Atlantic, *J. Geophys. Res.*, *109*, D24215, doi:10.1029/2004JD005137.

Chebbi, A., and P. Carlier (1996), Carboxylic acids in the troposphere, occurrence, sources, and sinks: A review, *Atmos. Environ.*, *30*(24), 4233–4249, doi:10.1016/1352-2310(96)00102-1.

Collett, J., A. Bator, X. Rao, and B. Demoz (1994), Acidity variations across the cloud drop size spectrum and their influence on rates of atmospheric sulfate production, *Geophys. Res. Lett.*, *21*(22), 2393–2396, doi:10.1029/94GL02480.

Crahan, K. K., D. Hegg, D. S. Covert, and H. Jonsson (2004), An exploration of aqueous oxalic acid production in the coastal marine atmosphere, *Atmos. Environ.*, *38*, 3757–3764, doi:10.1016/j.atmosenv.2004.04.009.

Ervens, B., and R. Volkamer (2010), Glyoxal processing by aerosol multiphase chemistry: Towards a kinetic modeling framework of secondary organic aerosol formation in aqueous particles, *Atmos. Chem. Phys.*, *10*(17), 8219–8244, doi:10.5194/acp-10-8219-2010.

Ervens, B., et al. (2003a), CAPRAM 2.4(MODAC mechanism): An extended and condensed tropospheric aqueous phase mechanism and its application, *J. Geophys. Res.*, *108*(D14), 4426, doi:10.1029/2002JD002202.

Ervens, B., S. Gligorovski, and H. Herrmann (2003b), Temperature-dependent rate constants for hydroxyl radical reactions with organic compounds in aqueous solutions, *Phys. Chem. Chem. Phys.*, *5*(9), 1811–1824, doi:10.1039/b300072a.

Ervens, B., G. Feingold, G. J. Frost, and S. M. Kreidenweis (2004), A modeling study of aqueous production of dicarboxylic acids: 1. Chemical pathways and speciated organic mass production, *J. Geophys. Res.*, *109*, D15205, doi:10.1029/2003JD004387.

Facchini, M. C., et al. (2008a), Important source of marine secondary organic aerosol from biogenic amines, *Environ. Sci. Technol.*, *42*(24), 9116–9121, doi:10.1021/es8018385.

Facchini, M. C., et al. (2008b), Primary submicron marine aerosol dominated by insoluble organic colloids and aggregates, *Geophys. Res. Lett.*, *35*, L17814, doi:10.1029/2008GL034210.

Feingold, G., and S. Kreidenweis (2000), Does cloud processing of aerosol enhance droplet concentrations?, *J. Geophys. Res.*, *105*(D19), 24,351–24,361, doi:10.1029/2000JD900369.

Fu, T.-M., D. J. Jacob, F. Wittrock, J. P. Burrows, M. Vrekoussis, and D. K. Henze (2008), Global budgets of atmospheric glyoxal and methylglyoxal, and implications for formation of secondary organic aerosols, *J. Geophys. Res.*, *113*, D15303, doi:10.1029/2007JD009505.

Galloway, M. M., P. S. Chhabra, W. H. Chan, J. D. Surratt, R. C. Flagan, J. H. Seinfeld, and F. N. Keutsch (2009), Glyoxal uptake on ammonium sulphate seed aerosol: Reaction products and reversibility of uptake under dark and irradiated conditions, *Atmos. Chem. Phys.*, *9*(10), 3331–3345, doi:10.5194/acp-9-3331-2009.

Gottwald, M., et al. (2006), SCIAMACHY, Monitoring the Changing Earth's Atmosphere, German Aerosp. Cent., Oberpfaffenhofen-Wessling, Germany.

Graedel, T. E., and C. J. Weschler (1981), Chemistry within aqueous atmospheric aerosols and raindrops, *Rev. Geophys.*, *19*(4), 505, doi:10.1029/RG019i004p00505.

Hopkins, R. J., Y. Desyaterik, A. V. Tivanski, R. A. Zaveri, C. M. Berkowitz, T. Tyliszczak, M. K. Gilles, and A. Laskin (2008), Chemical speciation of sulfur in marine cloud droplets and particles: Analysis of individual particles from the marine boundary layer over the California current, *J. Geophys. Res.*, *113*, D04209, doi:10.1029/2007JD008954.

Hsieh, L.-Y., S.-C. Kuo, C.-L. Chen, and Y. I. Tsai (2007), Origin of low-molecular-weight dicarboxylic acids and their concentration and size distribution variation in suburban aerosol, *Atmos. Environ.*, *41*(31), 6648–6661, doi:10.1016/j.atmosenv.2007.04.014.

Kawamura, K., and F. Sakaguchi (1999), Molecular distributions of water soluble dicarboxylic acids in marine aerosols over the Pacific Ocean including tropics, *J. Geophys. Res.*, *104*(D3), 3501–3509, doi:10.1029/1998JD100041.

Kawamura, K., H. Kasukabe, and L. A. Barrie (1996a), Source and reaction pathways ofdicarboxylic acids, ketoacids and dicarbonyls in arctic aerosols at polar sunrise, *Atmos. Environ.*, *30*, 1709–1722, doi:10.1016/1352-2310(95)00395-9.

Kawamura, K., R. Semèrè, Y. Imai, Y. Fujii, and M. Hayashi (1996b), Water soluble dicarboxylic acids and related compounds in Antarctic aerosols, *J. Geophys. Res.*, *101*(D13), 18,721–18,728, doi:10.1029/96JD01541.

Kawamura, K., H. Kasukabe, and L. A. Barrie (2010), Secondary formation of water-soluble organic acids and α-dicarbonyls and their contributions to total carbon and water-soluble organic carbon: Photochemical aging of organic aerosols in the Arctic spring, *J. Geophys. Res.*, *115*, D21306, doi:10.1029/2010JD014299.

Keene, W. C., R. Sander, A. A. P. Pszenny, R. Vogt, P. J. Crutzen, and J. N. Galloway (1998), Aerosol Ph in the marine boundary layer: A review and model evaluation, *J. Aerosol Sci.*, *29*(3), 339–356, doi:10.1016/S0021-8502(97)10011-8.

Keene, W. C., A. A. P. Pszenny, J. R. Maben, and R. Sander (2002), Variation of marine aerosol acidity with particle size, *Geophys. Res. Lett.*, *29*(7), 1101, doi:10.1029/2001GL013881.

Keene, W. C., A. A. P. Pszenny, J. R. Maben, E. Stevenson, and A. Wall (2004), Closure evaluation of size-resolved aerosol pH in the New England coastal atmosphere during summer, *J. Geophys. Res.*, *109*, D23307, doi:10.1029/2004JD004801.

Keene, W. C., et al. (2007), Chemical and physical characteristics of nascent aerosols produced by bursting bubbles at a model air-sea interface, *J. Geophys. Res.*, *112*, D21202, doi:10.1029/2007JD008464.

Kerminen, V.-M., K. Teinilä, R. Hillamo, and T. Mäkelä (1999), Size-segregated chemistry of particulate dicarboxylic acids in the Arctic atmosphere, *Atmos. Environ.*, *33*, 2089–2100, doi:10.1016/S1352-2310(98)00350-1.

Kerminen, V.-M., C. Ojanen, T. Pakkanen, R. Hillamo, M. Aurela, and J. Meriläinen (2000), Low-molecular-weight dicarboxylic acids in an urban and rural atmosphere, *J. Aerosol Sci.*, *31*(3), 349–362, doi:10.1016/S0021-8502(99)00063-4.

Liggio, J., S.-M. Li, and R. Mclaren (2005), Heterogeneous reactions of glyoxal on particulate matter: Identification of acetals and sulfate esters, *Environ. Sci. Technol.*, *39*(6), 1532–1541, doi:10.1021/es048375y.

Lim, H.-J., A. G. Carlton, and B. J. Turpin (2005), Isoprene forms secondary organic aerosol through cloud processing: Model simulations, *Environ. Sci. Technol.*, *39*(12), 4441–4446, doi:10.1021/es048039h.

Matsumoto, K., I. Nagao, H. Tanaka, H. Miyaji, T. Iida, and Y. Ikebe (1998), Seasonal characteristics of organic and inorganic species and their size distributions in atmospheric aerosols over the northwest Pacific Ocean, *Atmos. Environ.*, *32*(11), 1931–1946, doi:10.1016/S1352-2310(97)00499-8.

Miyazaki, Y., K. Kawamura, and M. Sawano (2010), Size distributions and chemical characterization of water soluble organic aerosols over the western North Pacific in summer, *J. Geophys. Res.*, *115*, D23210, doi:10.1029/2010JD014439.

Mochida, M., A. Kawabata, and K. Kawamura (2003a), Seasonal variation and origins of dicarboxylic acids in the marine atmosphere over the western North Pacific, *J. Geophys. Res.*, *108*(D6), 4193, doi:10.1029/2002JD002355.

Mochida, M., N. Umemoto, K. Kawamura, and M. Uematsu (2003b), Bimodal size distribution of C2–C4 dicarboxylic acids in the marine aerosols, *Geophys. Res. Lett.*, *30*(13), 1672, doi:10.1029/2003GL017451.

Monks, P., G. Salisbury, G. Holland, S. Pnkett, and G. Ayers (2000), A seasonal comparison of ozone photochemistry in the remote marine boundary layer, *Atmos. Environ.*, *34*(16), 2547–2561, doi:10.1016/S1352-2310(99)00504-X.

Myriokefalitakis, S., M. Vrekoussis, K. Tsigaridis, F. Wittrock, A. Richter, C. Brühl, R. Volkamer, J. P. Burrows, and M. Kanakidou (2008), The influence of natural and anthropogenic secondary sources on the glyoxal global distribution, *Atmos. Chem. Phys.*, *8*, 4965–4981, doi:10.5194/acp-8-4965-2008.

O'Dowd, C. D., M. C. Facchini, F. Cavalli, D. Ceburnis, M. Mircea, S. Decesari, S. Fuzzi, Y. J. Yoon, and J.-P. Putaud (2004), Biogenically driven organic contribution to marine aerosol, *Nature*, *431*, 676–680, doi:10.1038/nature02959.

Okuzawa, K., M. Mochida, J. Bendle, H. Wang, and K. Kawamura (2007), Diurnal variation of semi-volatile dicarbonyls and hydroxycarbonyls in the urban atmosphere, *Chikyukagaku* (*Geochemistry*), *41*, 125–134.

Perri, M. J., S. Seitzinger, and B. J. Turpin (2009), Secondary organic aerosol production from aqueous photooxidation of glycolaldehyde: Laboratory experiments, *Atmos. Environ.*, *43*, 1487–1497, doi:10.1016/j.atmosenv.2008.11.037.

Platt, U. (1994), Differential optical absorption spectroscopy (DOAS), in *Air Monitoring by Spectroscopic Techniques*, edited by M. W. Sigrist, pp. 27–84, John Wiley, New York.

Reeser, D. I., C. George, and D. J. Donaldson (2009a), Photooxidation of halides by chlorophyll at the air-salt water interface, *J. Phys. Chem. A*, *113*(30), 8591–8595, doi:10.1021/jp903657j.

Reeser, D. I., A. Jammoul, D. Clifford, M. Brigante, C. George, and D. J. Donaldson (2009b), Photoenhanced reaction of ozone with chlorophyll at the seawater surface, *J. Phys. Chem. C*, *113*, 2071–2077, doi:10.1021/jp805167d.

Rinaldi, M., et al. (2009), On the representativeness of coastal aerosol studies to open ocean studies: Mace Head – A case study, *Atmos. Chem. Phys.*, *9*, 9635–9646, doi:10.5194/acp-9-9635-2009.

Rinaldi, M., S. Decesari, E. Finessi, L. Giulianelli, C. Carbone, S. Fuzzi, C. D. O'Dowd, D. Ceburnis, and M. C. Facchini (2010), Primary and secondary organic marine aerosol and oceanic biological activity: Recent results and new perspectives for future studies, *Adv. Meteorol.*, *310682*, doi:10.1155/2010/310682.

Rozanov, A., V. Rozanov, M. Buchwitz, A. Kokhanovsky, and J. P. Burrows (2005), SCIATRAN 2.0–A new radiative transfer model for geophysical applications in the 175–2400 nm spectral region, *Adv. Space Res.*, *36*(5), 1015–1019, doi:10.1016/j.asr.2005.03.012.

Sciare, J., M. Kanakidou, and N. Mihalopoulos (2000), Diurnal and seasonal variation of atmospheric dimethylsulfoxide at Amsterdam Island in the southern Indian Ocean, *J. Geophys. Res.*, *105*(D13), 17,257–17,265, doi:10.1029/1999JD901186.

Sciare, J., H. Cachier, R. Sarda-Estève, T. Yu, and X. Wang (2007), Semi-volatile aerosols in Beijing (R.P. China): Characterization and influence on various PM 2.5 measurements, *J. Geophys. Res.*, *112*, D18202, doi:10.1029/2006JD007448.

Sciare, J., O. Favez, K. Oikonomou, H. Cachier, and V. Kazan (2009), Long-term observations of carbonaceous aerosols in the Austral Ocean atmosphere: Evidence of a biogenic marine organic source, *J. Geophys. Res.*, *114*, D15302, doi:10.1029/2009JD011998.

Shapiro, E. L., J. Szprengiel, N. Sareen, C. N. Jen, M. R. Giordano, and V. F. McNeill (2009), Light-absorbing secondary organic material formed by glyoxal in aqueous aerosol mimics, *Atmos. Chem. Phys.*, *9*, 2289–2300, doi:10.5194/acp-9-2289-2009.

Sinreich, R., R. Volkamer, F. Filsinger, U. Frieß, C. Kern, U. Platt, O. Sebastiàn, and T. Wagner (2007), MAX-DOAS detection of glyoxal during ICARTT 2004, *Atmos. Chem. Phys.*, *7*, 1293–1303, doi:10.5194/acp-7-1293-2007.

Sinreich, R., S. Coburn, B. Dix, and R. Volkamer (2010), Ship-based detection of glyoxal over the remote tropical Pacific Ocean, *Atmos. Chem. Phys.*, *10*, 11,359–11,371, doi:10.5194/acp-10-11359-2010.

Sorooshian, A., et al. (2006), Oxalic acid in clear and cloudy atmospheres: Analysis of data from International Consortium for Atmospheric Research on Transport and Transformation 2004, *J. Geophys. Res.*, *111*, D23S45, doi:10.1029/2005JD006880.

Sorooshian, A., M.-L. Lu, F. J. Brechtel, H. Jonsson, G. Feingold, R. C. Flagan, and J. H. Seinfeld (2007), On the source of organic acid aerosol layers above clouds, *Environ. Sci. Technol.*, *41*(13), 4647–4654, doi:10.1021/es0630442.

Tan, Y., M. J. Perri, S. P. Seitzinger, and B. J. Turpin (2009), Effects of precursor concentration and acidic sulfate in aqueous glyoxal-OH radical oxidation and implications for secondary organic aerosol, *Environ. Sci. Technol.*, *43*(21), 8105–8112, doi:10.1021/es901742f.

Turekian, V. C., S. A. Macko, and W. C. Keene (2003), Concentrations, isotopic compositions, and sources of size-resolved, particulate organic carbon and oxalate in near-surface marine air at Bermuda during spring, *J. Geophys. Res.*, *108*(D5), 4157, doi:10.1029/2002JD002053.

Von Glasow, R., and P. J. Crutzen (2004), Model study of multiphase DMS oxidation with a focus on halogens, *Atmos. Chem. Phys.*, *4*(3), 589–608, doi:10.5194/acp-4-589-2004.

Vrekoussis, M., F. Wittrock, A. Richter, and P. J. Burrows (2009), Temporal and spatial variability of glyoxal as observed from space, *Atmos. Chem. Phys.*, *9*, 4485–4504, doi:10.5194/acp-9-4485-2009.

Vrekoussis, M., F. Wittrock, A. Richter, and J. P. Burrows (2010), GOME-2 observations of oxygenated VOCs: What can we learn from the ratio glyoxal to formaldehyde on a global scale?, *Atmos. Chem. Phys.*, *10*, 10,145–10,160, doi:10.5194/acp-10-10145-2010.

Warneck, P. (2003), In-cloud chemistry opens pathway to the formation of oxalic acid in the marine atmosphere, *Atmos. Environ.*, *37*, 2423–2427, doi:10.1016/S1352-2310(03)00136-5.

Wittrock, F., A. Richter, H. Oetjen, J. P. Burrows, M. Kanakidou, S. Myriokefalitakis, R. Volkamer, S. Beirle, U. Platt, and T. Wagner (2006), Simultaneous global observations of glyoxal and formaldehyde from space, *Geophys. Res. Lett.*, *33*, L16804, doi:10.1029/2006GL026310.

Yao, X., M. Fang, and C. K. Chan (2002), Size distributions and formation of dicarboxylic acids in atmospheric particles, *Atmos. Environ.*, *36*, 2099–2107.

Yu, L., M. Shulman, R. Kopperud, and L. Hildemann (2005), Fine organic aerosols collected in a humid, rural location (Great Smoky Mountains, Tennessee, USA): Chemical and temporal characteristics, *Atmos. Environ.*, *39*(33), 6037–6050, doi:10.1016/j.atmosenv.2005.06.043.

Zhou, X., and K. Mopper (1990), Apparent partition coefficients of 15 carbonyl compounds between air and seawater and between air and freshwater; implications for air-sea exchange, *Environ. Sci. Technol.*, *24*(12), 1864–1869, doi:10.1021/es00082a013.

Zhou, X., and K. Mopper (1997), Photochemical production of low-molecular-weight carbonyl compounds in seawater and surface microlayer and their air-sea exchange, *Mar. Chem.*, *56*, 201–213, doi:10.1016/S0304-4203(96)00076-X.

J. P. Burrows, Institute of Environmental Physics and Remote Sensing, University of Bremen, NW1, PO Box 33 04 40, D-28334 Bremen, Germany.

C. Carbone, S. Decesari, M. C. Facchini, E. Finessi, S. Fuzzi, and M. Rinaldi, Institute of Atmospheric Sciences and Climate, National Research Council, via P. Gobetti 101, I-40129 Bologna, Italy. (m.rinaldi@isac.cnr.it)

D. Ceburnis and C. D. O'Dowd, School of Experimental Physics, National University of Ireland Galway, University Road, Galway, Ireland.

B. Ervens, Chemical Sciences Division, Earth System Research Laboratory, NOAA, 325 Broadway, Boulder, CO 80305, USA.

J. Sciare, Laboratoire des Sciences du Climat et de l'Environnement, CNRS-CEA-IPSL, F-91191 Gif-sur-Yvette, France.

K. Tsigaridis, NASA Goddard Institute for Space Studies, 2880 Broadway, New York, NY 10025, USA.

M. Vrekoussis, Research Centre for Atmospheric Physics and Climatology, Academy of Athens, 24 Omirou str., GR-10672 Athens, Greece.